



Thermodynamic destabilization and aggregation propensity as the mechanism behind the association of apoE3 mutants and lipoprotein glomerulopathy

Maria Katsarou,* Efstratios Stratikos,^{1,†} and Angeliki Chroni^{1,*}

Institute of Biosciences and Applications,* and Protein Chemistry Laboratory, Institute of Nuclear & Radiological Sciences and Technology, Energy & Safety (INRaSTES),[†] National Centre for Scientific Research “Demokritos,” Agia Paraskevi, Athens 15341, Greece

Abstract Lipoprotein glomerulopathy (LPG) is a rare renal disease, characterized by lipoprotein thrombi in glomerular capillaries. A series of apoE mutations have been associated with LPG development. We previously showed that three mutants based on apoE3 sequence, in which an arginine was substituted by proline, are thermodynamically destabilized and aggregation-prone. To examine whether other LPG-associated apoE3 mutations induce similar effects, we characterized three nonproline LPG-associated apoE3 mutations, namely, R25C (apoE_{Kyoto}), R114C (apoE_{Tsukuba}), and A152D (apoE_{LasVegas}). All three apoE3 variants are found to have significantly reduced helical content and to be thermodynamically destabilized, both in lipid-free and lipoprotein-associated form, and to expose a larger portion of hydrophobic surface to the solvent compared with WT apoE3. Furthermore, all three apoE3 variants are aggregation-prone, as shown by dynamic light-scattering measurements and by their enhanced capacity to bind the amyloid probe thioflavin T. Overall, our data suggest that the LPG-associated apoE3 mutations R25C, R114C, and A152D induce protein misfolding, which may contribute to protein aggregation in glomerular capillaries. The similar effects of both LPG-associated proline and nonproline mutations on apoE3 structure suggest that the thermodynamic destabilization and enhanced aggregation of apoE3 may constitute a common underlying mechanism behind the pathogenesis of LPG.—Katsarou, M., E. Stratikos, and A. Chroni. Thermodynamic destabilization and aggregation propensity as the mechanism behind the association of apoE3 mutants and lipoprotein glomerulopathy. *J. Lipid Res.* 2018. 59: 2339–2348.

Supplementary key words apolipoproteins • dyslipidemias • kidney • physical biochemistry • apolipoprotein E • mutations • thermodynamic stability

Lipoprotein glomerulopathy (LPG) is a rare renal disease, characterized by distinctive lipoprotein thrombi in

the glomerular capillaries, often abnormal lipid profile, proteinuria, and progressive kidney failure (1, 2). The relapse of LPG following kidney transplantation in LPG patients (3, 4) has suggested that factors outside the kidney should be crucial for the disease pathogenesis. One such factor has been proposed to be mutated apoE, because LPG has been related with inherited mutations within the *apoE* gene that act in a dominant way but with incomplete penetrance (1, 2, 5, 6).

ApoE is a major protein component of the lipoprotein transport system and plays critical roles in dyslipidemia and atherosclerosis (7, 8). Human apoE has three common isoforms, the apoE2, apoE3, and apoE4, each differing in the amino acid positions 112 and 158 (9). The polymorphic background and mutations in the *apoE* gene have been linked with the pathogenesis of several diseases related to lipid metabolism, such as type III hyperlipoproteinemia, atherosclerosis, diabetic dyslipidemia, and LPG, as well as of neurodegenerative disorders, such as Alzheimer's disease (5, 6, 8, 10, 11).

ApoE is highly helical with labile tertiary structure (12) that can undergo significant conformational changes during its physiological functions that include lipid binding, protein-protein interactions, and other processes (10, 13–16). Lipid-free apoE is folded into two structural domains, an N-terminal and a carboxyl-terminal, connected with a hinge region (10, 13–16). Crystal structure analysis of the N-terminal domain of apoE showed that this domain folds as a four-helix bundle of amphipathic α -helices (17). NMR analysis of full-length apoE also showed a four-helix bundle in the N-terminal domain, as well as two helices in the hinge region and three helices in the carboxyl-terminal

Abbreviations: ANS, 1-anilinonaphthalene-8-sulfonic acid; CD, circular dichroism; DLS, dynamic light scattering; GndHCl, guanidine hydrochloride; LPG, lipoprotein glomerulopathy; PC, 1-palmitoyl-2-oleoyl-sn-glycero-3-phosphocholine; ThT, thioflavin T.

¹To whom correspondence should be addressed.
e-mail: achroni@bio.demokritos.gr (A.C.);
stratos@rrp.demokritos.gr (E.S.)

This work was supported in part by Ministry of National Education and Religious Affairs Grant THALIS MIS 377286 and by the Hellenic Society of Lipidology, Atherosclerosis and Vascular Disease.

Manuscript received 25 July 2018 and in revised form 11 October 2018.

Published, JLR Papers in Press, October 11, 2018

DOI <https://doi.org/10.1194/jlr.M088732>

Copyright © 2018 Katsarou et al. Published under exclusive license by The American Society for Biochemistry and Molecular Biology, Inc.

This article is available online at <http://www.jlr.org>

domain (14). Interactions between the amino- and carboxyl-terminal regions of apoE are proposed to affect the overall folding of the protein. Additionally, it has been shown that apoE contains intrinsically disordered regions and smaller flexible regions that surround structured helices, affecting the conformation and functional properties of apoE (14–16). Several biophysical studies have shown that apoE displays low thermodynamic stability and significant conformational plasticity, and allelic differences as well as single point mutations have been shown to affect protein conformation and to hinder physiological function (13, 15, 16, 18–20). Furthermore, apoE has been shown to be prone to aggregation and to form oligomeric structures in solution (21, 22).

The majority of LPG-associated apoE mutations are located in the helical N-terminal domain of the molecule (5, 6). Most LPG patients are heterozygous for the apoE mutations and have elevated plasma apoE levels (5, 6, 23–25). Initially, apoE mutations were discovered in patients from East Asian countries, and it was believed that the disease was restricted in those areas, but several LPG cases and apoE mutations have been reported in patients of Caucasian ancestry in Europe and the United States (1). The direct relation of apoE mutations with LPG has been supported by gene transfer studies of apoE_{Sendai} (R145P), the second more frequent apoE mutant detected in LPG patients, to apoE-deficient mice that lead to lipoprotein depositions in the glomerulus of the kidney (26). These findings suggested that apoE dysfunction may be an etiologic cause of LPG, although the exact mechanism remains elusive.

In an effort to gain mechanistic insight linking the presence of apoE mutations and the development of LPG, we previously examined the effects of three Arg to Pro substitutions at positions 145, 147, and 158 of the apoE3 sequence on structural and conformational integrity of protein. We showed that apoE3 variants carrying these mutations [R145P (apoE_{Sendai}), R147P (apoE_{Chicago}), and R158P (apoE_{Osaka} or apoE_{Kurashiki})] displayed major thermodynamic destabilization, structural perturbations, and increased hydrophobic surface exposure to the solvent and were aggregation prone (18). These findings suggested that the folding defects and aggregation propensity of LPG-associated apoE mutations may constitute a component of the disease pathogenic mechanism. Because, however, proline reduces the helical content of apoE3, it is possible that these destabilization effects are limited to the proline mutations and not to other known LPG-associated apoE3 mutants. To test the generality of this mechanism, we set forth to examine whether substitutions of apoE3 amino acids with residues that are, in principle, compatible with helical secondary structure may also lead to perturbations in apoE structure and function. We therefore evaluated the effect of three other LPG-associated mutations based on apoE3 sequence, namely, R25C (apoE_{Kyoto}) (1, 27), which has been reported in various parts of the world and is the most common apoE mutation in LPG (1), R114C (apoE_{Tsukuba}) (28), and A152D (apoE_{LasVegas}) (29), on the structural, thermodynamic, and aggregation properties of the protein.

Here, we demonstrate that the three LPG-associated apoE3 mutants, R25C (apoE_{Kyoto}), R114C (apoE_{Tsukuba}), and A152D (apoE_{LasVegas}), display structural and thermodynamic perturbations both in lipid-free and lipoprotein-associated forms and expose a larger portion of hydrophobic surface to the solvent as compared with WT apoE3, as it was previously observed for R145P (apoE_{Sendai}), R147P (apoE_{Chicago}), and R158P (apoE_{Osaka} or apoE_{Kurashiki}) mutants (18). In addition, the three apoE3 mutants are aggregation prone, similarly to LPG-associated apoE3 mutants studied previously (18). Overall, our data indicate the presence of common themes in the dysfunction of LPG-associated apoE3 mutants that are related to structural and thermodynamic perturbations of protein, pointing toward a unifying mechanism contributing to LPG pathogenesis.

MATERIALS AND METHODS

Site-directed mutagenesis

The pET32-E33C vector containing a Trx tag, a 6× His-tag, and a 3C-protease site at the fusion junction with the human cDNA for full-length apoE3 has been described previously (18). The R25C, R114C, and A152D mutations were introduced into the gene of *apoE3* by site-directed mutagenesis, by using the QuikChange II XL site-directed mutagenesis kit (Agilent, Santa Clara, CA), according to the manufacturer's instructions. The sequences of primers used for mutagenesis were: R25C: 5'-GTG GCA GAG CGG CCA GTG CTG GGA ACT GGC ACT GG-3' and 5'-CCA GTG CCA GTT CCC AGC ACT GGC CGC TCT GCC AC-3'; R114C: 5'-GGA GGA CGT GTG CGG CTG CCT GGT GCA GTA CCG CG-3' and 5'-CGC GGT ACT GCA CCA GGC AGC CGC ACA CGT CCT CC-3'; and A152D: 5'-GCG CCT CCT CCG CGA TGA CGA TGA CCT GCA GAA GC-3' and 5'-GCT TCT GCA GGT CAT CGT CAT CGC GGA GGA GCC GC-3'. Successful mutagenesis was confirmed by DNA sequencing.

Expression and purification of WT and mutant apoE3 forms

The expression and purification of WT apoE3, as well as of mutant apoE3 forms R145P and R158P, was carried out as described previously (18). The production of mutant apoE3 forms R25C, R114C, and A152D was performed using the same protocol. Briefly, BL21-Gold (DE3) cells (Stratagene, Cedar Creek, TX) were transformed with the vectors, and the recombinant proteins expression was induced with isopropyl-β-D-thiogalactopyranoside. All Trx-fused proteins were expressed soluble and purified by Ni-nitrilotriacetic acid (Ni-NTA) resin (Thermo Scientific, Rockford, IL) affinity chromatography following elution by increasing concentrations of imidazole (18). The Trx-tag was subsequently cleaved from apoE by His-tagged 3C protease, prepared using the pET-24/His-3C vector kindly provided by Dr. Arie Geerloff (EMBL, Heidelberg, Germany), and the released apoE was isolated by a second Ni-NTA resin affinity chromatography step in the flow-through (18). After purification, each apoE form was extensively dialyzed against 5 mM NH₄HCO₃, lyophilized, and stored at -80°C. Before analyses, the lyophilized proteins were dissolved in 6 M guanidine hydrochloride (GndHCl) in 50 mM sodium phosphate buffer, pH 7.4, containing 1 mM DTT and refolded by extensive dialysis against the same buffer (50 mM sodium phosphate buffer, pH 7.4, and 1 mM DTT). The samples were then centrifuged at 12,000 g for 20 min, at 4°C, to remove any precipitated protein. The refolded proteins were approximately 98% pure, as

estimated by SDS-PAGE. All analyses were performed on freshly refolded proteins.

Preparation of reconstituted apoE-phosphatidylcholine-cholesterol particles

Reconstituted discoidal lipoprotein particles containing WT or mutant apoE3 forms were prepared, using 1-palmitoyl-2-oleoyl-sn-glycero-3-phosphocholine (PC):cholesterol:apoE:sodium cholate in 50 mM sodium phosphate buffer (pH 7.4) and 1 mM DTT at a molar ratio of 100:10:1:100, as described (18, 30). All lipoprotein samples were prepared using the same phospholipid-cholesterol suspension, and the procedure was performed in parallel. Particles were stored at 4°C under N₂ to prevent lipid oxidation.

Circular dichroism spectroscopy

Far-UV circular dichroism (CD) spectra were recorded from 190 to 260 nm at 20°C with a Jasco 715 spectropolarimeter, and the spectra were collected as described before (18, 30). The concentration of lipid-free WT and mutant apoE3 forms was 0.08–0.1 mg/ml in 50 mM sodium phosphate buffer (pH 7.4) and 1 mM DTT and of the protein component (apoE3 forms) of lipoprotein particles was 0.1 mg/ml in 50 mM sodium phosphate buffer (pH 7.4). Helical content was calculated using the molecular ellipticity at 222 nm (31) by the equation:

$$\% \alpha - \text{helix} = \left(-[\Theta]_{222} + 3000 \right) / (36000 + 3000) \times 100.$$

For thermal denaturation analysis of lipid-free apoE3 forms, the change in molar ellipticity at 222 nm was monitored while varying the temperature from 20°C to 80°C at a rate of 1°C/min. The thermal denaturation curve was fitted to a Boltzmann simple sigmoidal model using the GraphPad Prism™ software (GraphPad Software Inc., La Jolla, CA). The apparent melting temperature T_m was determined by the sigmoidal fit as midpoint of the thermal transition. The relative enthalpy change was calculated as described previously (18, 32). For thermal denaturation analysis of lipoprotein particles, all measuring parameters were identical to that of the lipid-free apoE3 forms, with the exception of the temperature range that varied from 20°C to 100°C.

Chemical denaturation experiments

To record the chemical denaturation profile of lipid-free apoE3 forms (0.07 mg/ml in 50 mM sodium phosphate buffer, pH 7.4, and 1 mM DTT) we measured the changes in intrinsic tryptophan fluorescence (excitation 295 nm, emission 340 nm) of the proteins upon increasing concentrations of GndHCl by adding various amounts of 8.0 M GndHCl, as described (18). The fluorescence signal of the sample was measured in a Quantamaster 4 fluorescence spectrometer (Photon Technology International, NJ). The experimental data were fitted to a three-state denaturation model, and the relative change in Gibbs-free energy corresponding to first, second, and total unfolding transition during the chemical denaturation was calculated as described (33, 34).

ANS fluorescence measurement

Lipid-free WT or mutant apoE3 forms (0.08 mg/ml in 50 mM sodium phosphate buffer, pH 7.4, and 1 mM DTT) were placed into the wells of a 96-well black microplate, mixed with 1-anilino-naphthalene-8-sulfonic acid (ANS; Sigma-Aldrich, St. Louis, MO) so that the final ANS concentration was 310 μM, and the fluorescence signal was measured by an Infinite M200 microplate reader (Tecan Group Ltd., Mannedorf, Switzerland) (18). The excitation wavelength was set at 395 nm and the emission range was from 425 to 600 nm. A control ANS spectrum in the absence of protein was also recorded to allow the calculation of ANS fluorescence enhancement in the presence of apoE3 forms.

DLS analysis

Dynamic light-scattering (DLS) experiments were performed using a Zetasizer nano series instrument (Malvern Instruments Ltd., UK) at 20°C. Lipid-free apoE3 forms at a concentration of 0.1 mg/ml in 50 mM sodium phosphate buffer, pH 7.4, and 1 mM DTT were analyzed immediately after their refolding and following incubation at 37°C for 24 h.

ThT fluorescence measurement

Thioflavin T (ThT) (Sigma-Aldrich) was dissolved into glycine 0.1 M, pH 8.5, at a concentration of 10 mM (ThT stock solution) and stored at 4°C. The day of the experiment, a working stock of ThT at concentration of 100 μM in glycine 0.1 M, pH 8.5, was prepared. Lipid-free WT or mutant apoE3 forms at a concentration of 0.4 mg/ml in Dulbecco's PBS (1.47 mM KH₂PO₄, 8.06 mM Na₂HPO₄·7H₂O, 2.67 mM KCl, and 137.96 mM NaCl, without Ca or Mg), pH 7.4, and 1 mM DTT were incubated at 37°C under mild rotation (40 rpm) for 24 h. Subsequently, 25 μl of protein sample was inserted into the wells of a 96-well microplate and mixed with 5 μl of ThT working stock solution to a final volume of 100 μl so that the final concentration of protein was 100 μg/ml and of ThT was 5 μM. The fluorescence signal of ThT was measured by an Infinite M200 microplate reader (Tecan Group Ltd.). The excitation wavelength was set at 430 nm, and the emission wavelength was 480 nm. Control ThT signal in buffer in the absence of protein was also recorded.

RESULTS

Protein expression and purification

To evaluate the effect of LPG-associated apoE3 mutations R25C, R114C, and A152D on structural and conformational properties of the protein, we expressed and

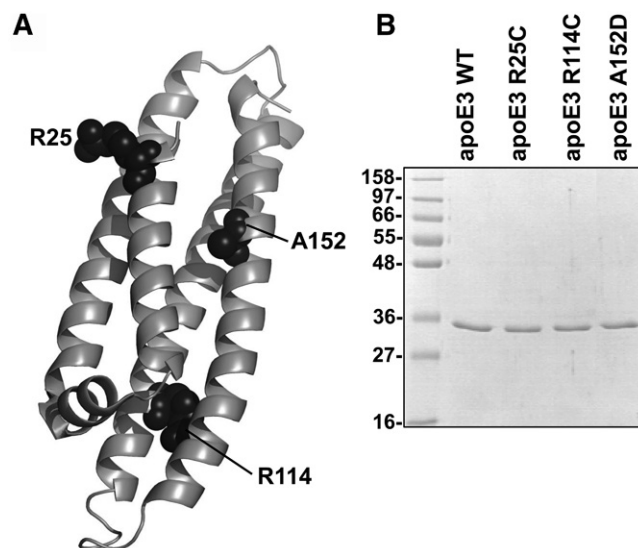


Fig. 1. Schematic of the crystal structure of the N-terminal domain of human apoE3 indicating the location of 25, 114, and 152 residues and SDS-PAGE analysis of purified WT and mutant R25C, R114C, and A152D apoE3 forms. A: The position of residues 25, 114, and 152 of apoE3 were mapped on the crystal structure of the N-terminal domain of apoE3 with Protein Data Bank ID code 1LPE. B: The refolded WT and mutant apoE3 forms, produced and purified as described in Materials and Methods, were subjected to electrophoresis on 15% SDS polyacrylamide gels that were stained with Coomassie Brilliant Blue.

purified recombinant apoE3 forms carrying each mutation, as well as WT apoE3, using an *Escherichia coli* expression system (18). All mutations are located on the N-terminal moiety of apoE3 (Fig. 1A). Following purification, the recombinant proteins were approximately 98% pure, as judged by SDS-PAGE analysis (Fig. 1B). Before each analysis presented below, all apoE3 forms were subjected in parallel to a refolding step as previously described (18). Proteins were refolded and kept in a reducing environment by the addition of 1 mM DTT, to avoid oxidation of cysteine residues.

Secondary structure of lipid-free WT and mutant apoE3 forms

Because all studied mutations are located within the helical segments of apoE3, we examined whether they affect the secondary structure of the protein. To test this, we recorded the CD spectra of lipid-free WT apoE3 and mutants and calculated the α -helical content of the protein. The CD spectrum of lipid-free apoE3 mutants was found to overall have a similar shape to the spectrum of WT apoE3 (Fig. 2A). The intensity of the molar ellipticity, however, was reduced in all apoE3 mutants, showing a significant loss of helicity, by at least 7%, as compared with WT apoE3, with the most pronounced helicity loss recorded for A152D (~13% loss) (Fig. 2B). Such reduction of α -helical content cannot solely be attributed to local perturbation of the helical structure due to the presence

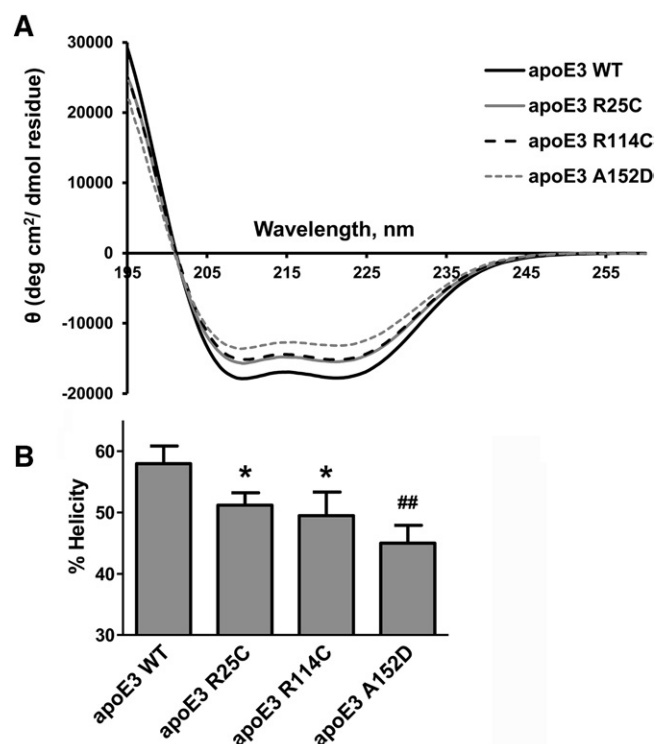


Fig. 2. Effect of R25C, R114C, and A152D mutations on the secondary structure of apoE3. A: Far-UV CD spectra of WT and mutant apoE3 forms. Spectra are averages of three separate experiments. B: Percent α -helical content calculated based on the molar ellipticity at 222 nm as described in Materials and Methods. Values represent the means \pm SD ($n = 3$). * $P < 0.05$; ## $P < 0.001$ versus apoE3 WT.

of the mutated residue and suggests that all mutations may exert more extended perturbations to the local or global folding of the protein.

Thermodynamic stability of lipid-free WT and mutant apoE3 forms

Because all apoE3 mutants display secondary structure perturbations, we proceeded to examine the thermodynamic stability of the protein. We compared the thermal denaturation profile of each mutant to that of WT apoE3, following the CD signal at 222 nm, while the protein was gradually unfolded by increasing the temperature of the sample from 20°C to 80°C (Fig. 3A–C). Although the thermal denaturation of apoE3 is a gradual multistate and not fully reversible process, such analysis has been used before as a method of comparing changes between apoE3 variants, primarily because the irreversible changes are relatively slow compared with the heat unfolding (34, 35). We therefore calculated the thermal midpoint of the transition, T_m , and the apparent enthalpy change of the transition, ΔH . R25C and A152D unfolded at a significantly lower temperature compared with WT apoE3 (Fig. 3D), and all three apoE3 mutants had statistically significant

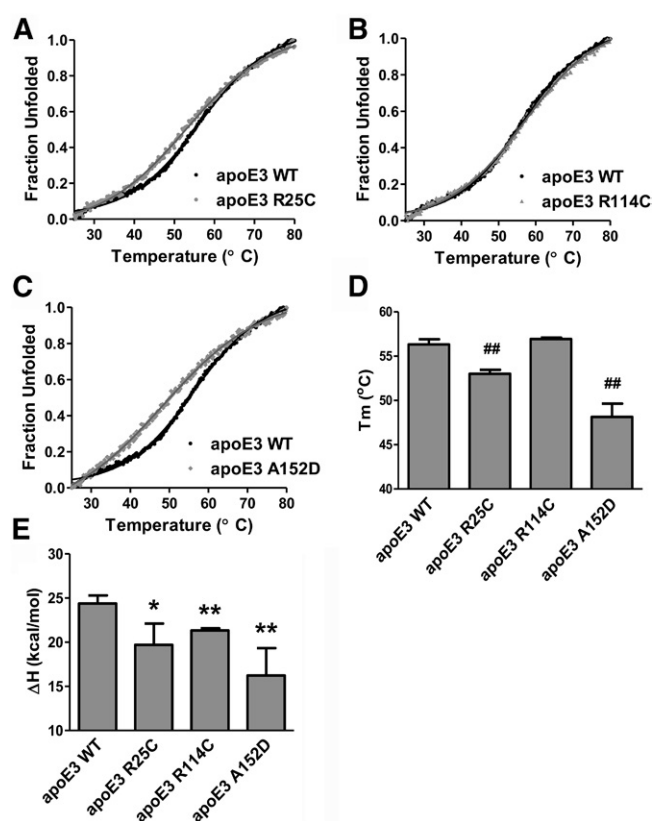


Fig. 3. Effect of R25C, R114C, and A152D mutations on thermal unfolding of apoE3. A–C: The thermal denaturation profile of each mutant is presented in comparison to the WT protein. The y axis has been normalized to correspond to the fraction of the protein in the unfolded state. Experimental data were fit to a simple two-state Boltzmann transition (solid line). D, E: Apparent T_m and ΔH values for the heating-induced transitions were calculated as described in Materials and Methods. Values represent the means \pm SD ($n = 3$). * $P < 0.05$; ** $P < 0.005$; ## $P < 0.001$ versus apoE3 WT.

lower apparent ΔH values as compared with WT protein (Fig. 3E).

To further investigate possible changes in the thermodynamic stability of apoE3 due to the presence of mutations R25C, R114C, and A152D, we compared the chemical denaturation profile of each mutant to that of WT apoE3. The tryptophan fluorescence signal of each mutant protein was followed as a function of increasing concentration of the chaotrope GndHCl (Fig. 4A–C). ApoE has been shown to undergo a two-phase unfolding transition when treated with GndHCl, with an unfolding intermediate appearing between 1 and 2 M (36). Modeling of the unfolding profile to a three-state denaturation model can be used to calculate apparent values for the change in Gibbs energy during unfolding (33, 34). All apoE3 mutants followed a two-phase unfolding transition, but their first unfolding transition phase was less cooperative and had a lower apparent ΔG value as compared with WT apoE3 (Fig. 4D).

Overall, the data from thermal and chemical denaturation analyses indicated that all apoE3 mutants studied display significant thermodynamic perturbations. Residues R25, R114, and A152 of apoE3 appear to have a role in the thermodynamic stability of apoE3.

Hydrophobic surfaces exposure to the solvent of WT and mutant apoE3 forms

To evaluate whether the introduction of the mutations affect the solvent-exposed hydrophobic surfaces of apoE3, we used the hydrophobic reporter probe ANS, which changes

its fluorescence properties when interacting with hydrophobic sites on apoE (18–20). All apoE3 mutations resulted in significantly higher ANS fluorescence compared with WT apoE3 (Fig. 5A, B), indicating an increase in the exposure of solvent-accessible hydrophobic areas of the protein in the presence of mutation. The magnitude of the effect was greater than expected for the local effect of a single amino acid substitution from charged to more hydrophobic (R25C and R114C) and the reverse for a hydrophobic to charged substitution (A152D), indicating that the introduction of the mutation has more global effects on the hydrophobic patch exposure for the protein.

Secondary structure and thermodynamic stability of WT and mutant apoE3 forms in reconstituted lipoprotein particles

The structural and thermodynamic differences between WT apoE3 and the apoE3 mutants in lipid-free form prompted us to investigate whether the presence of each mutation also affects the structural and thermodynamic properties of apoE3 in lipoprotein-associated form. CD spectroscopic analysis revealed that the apoE3 mutants R25C, R114C, and A152D have significantly lower α -helical content, even when in lipoprotein form, compared with WT apoE3 (Fig. 6A, B). Thermal denaturation measurements showed that all three apoE3 mutants display a perturbed thermal denaturation profile (Fig. 7A–C), which may indicate some conformational defects in apoE3 in lipoprotein particles because of the mutations.

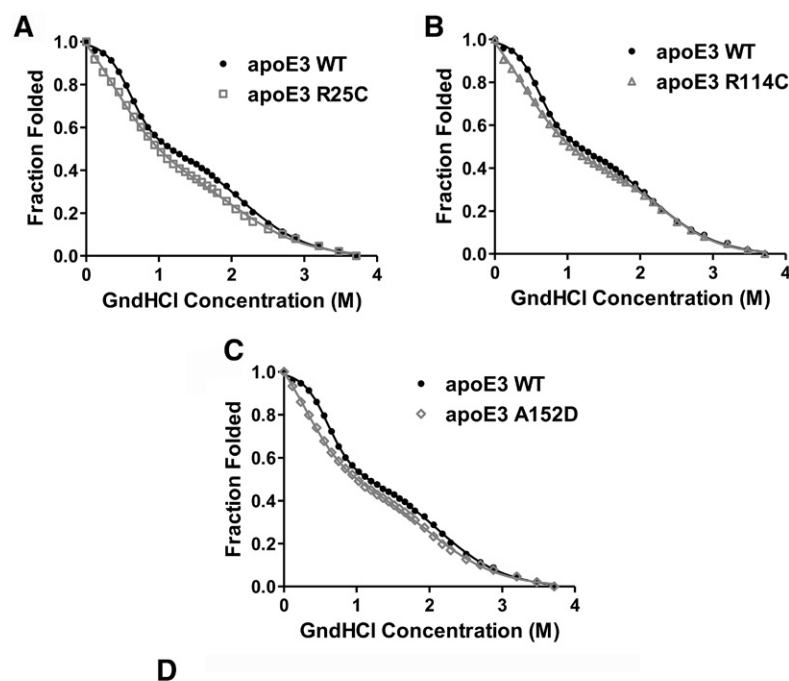


Fig. 4. Effect of R25C, R114C, and A152D mutations on chemical denaturation of apoE3. A–C: The chemical denaturation profile of each mutant is presented in comparison to the WT protein. The y axis has been normalized to correspond to the fraction of the protein that remains in the folded state. D: Experimental data were fitted to a three-state denaturation model [solid line (33)], and the apparent ΔG values for the transition between the folded state and the intermediate state (ΔG_1), between the intermediate state and the unfolded state (ΔG_2), and for the total transition between the folded state and the unfolded state (ΔG_{total}) were calculated as described in Materials and Methods. Values represent the means \pm SD ($n = 3$). * $P < 0.05$ versus apoE3 WT.

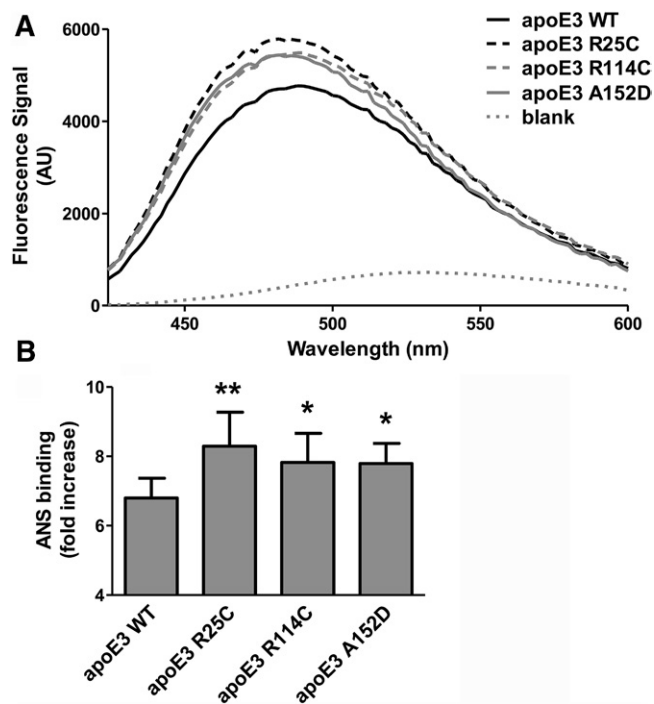


Fig. 5. Effect of R25C, R114C, and A152D mutations on solvent-exposed hydrophobic sites of apoE3. A: ANS fluorescence spectra in the presence or absence of WT apoE3 or mutant forms. Spectra are the average of four separate experiments. AU, arbitrary units. B: Fold increase in ANS fluorescence in the presence of WT apoE3 or mutant forms relative to free ANS in the same buffer. Values represent the means \pm SD ($n = 4$). * $P < 0.05$; ** $P < 0.005$ versus apoE3 WT.

Aggregation propensity of WT and mutant apoE3 forms

ApoE is known to be prone to self-association and to form oligomeric structures at higher concentrations (35, 37, 38). To examine whether the introduction of the mutations affects the oligomerization and/or aggregation of apoE3, we recorded the volume-normalized particle distribution profiles of WT and mutant apoE3 forms immediately after refolding and after their incubation at 37°C for 24 h by DLS (Fig. 8). Our analysis showed that, upon incubation at 37°C for 24 h, the three apoE3 mutants R25C, R114C, and A152D displayed a significant shift to larger hydrodynamic diameters as compared with their hydrodynamic diameter before incubation, in contrast to the WT apoE3, which was stable (Fig. 8A–D). The findings suggest that the mutations severely affect the oligomerization properties of apoE3 and make the mutant proteins more aggregation-prone at physiological temperatures.

Capacity of WT and mutant apoE3 forms to bind ThT

The finding that the LPG-associated apoE3 mutants R25C, R114C, and A152D have the tendency to aggregate following incubation at 37°C for 24 h, prompt us to examine whether these mutants can also bind to the amyloid probe ThT. ThT fluorescence intensity is low in aqueous solution, but it increases upon binding of the probe to amyloid aggregates and has been used previously to monitor the aggregation and amyloidogenic propensity of apolipoproteins (39, 40). ThT fluorescence was measured following incubation of apoE3 forms for 4, 24, and 48 h. Our analysis showed

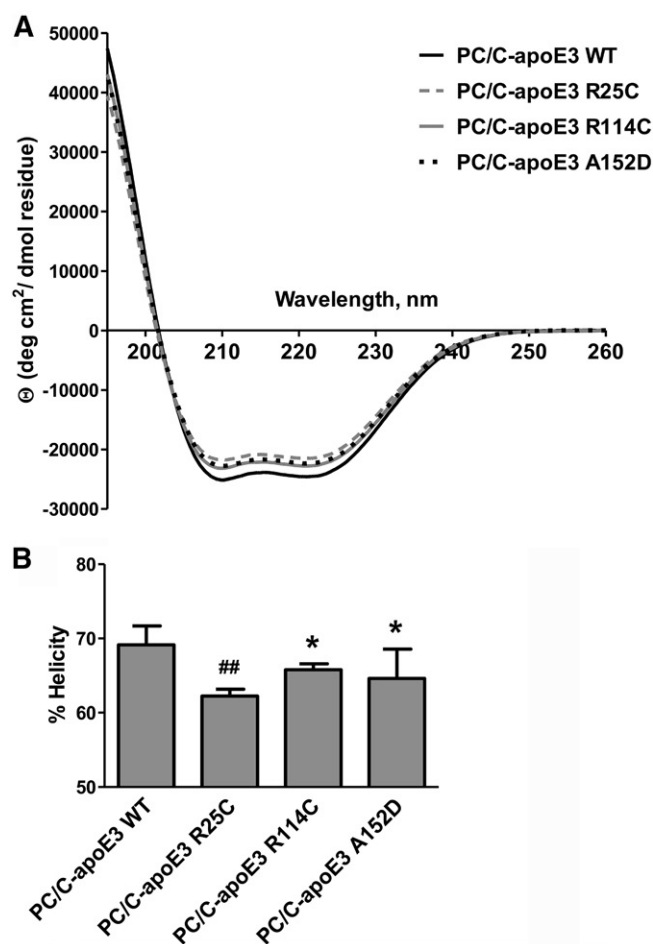


Fig. 6. Effect of R25C, R114C, and A152D mutations on the secondary structure of apoE3 in reconstituted lipoprotein particles. A: Far-UV CD spectra of PC/cholesterol (C)-apoE particles containing WT or mutant apoE3 forms. Spectra are averages of four separate experiments. B: Percent α -helical content of the protein component of lipoprotein particles calculated on the basis of the molar ellipticity at 222 nm, as described in Materials and Methods. Values represent the means \pm SD ($n = 4$). * $P < 0.005$; ## $P < 0.001$ versus apoE3 WT.

that the R25C, R114C, and A152D apoE3 mutants promoted much higher increase in ThT fluorescence signal as compared with WT apoE3 (Fig. 9). Specifically, incubation of apoE3 mutants for 4 h promoted a significant increase in ThT fluorescence as compared with WT apoE3. ThT fluorescence in the presence of apoE3 mutants, but not of WT apoE3, was further increased following incubation of proteins for 24 h. Incubation of WT apoE3 and apoE3 mutants for 48 h resulted in a similar increase of ThT fluorescence signal as the incubation for 24 h. Furthermore, our analysis showed that enhanced capacity for ThT binding also displayed, at all incubation times, the LPG-associated apoE3 mutants R145P and R158P (Fig. 9), which had been analyzed in a previous study by DLS and were likewise found to be oligomerized following their incubation at 37°C for 24 h (18). Based on these data and that of the DLS analysis, we conclude that the LPG-associated apoE mutations have a tendency to promote the formation of proamyloidogenic, possibly aggregated, large-size protein complexes.

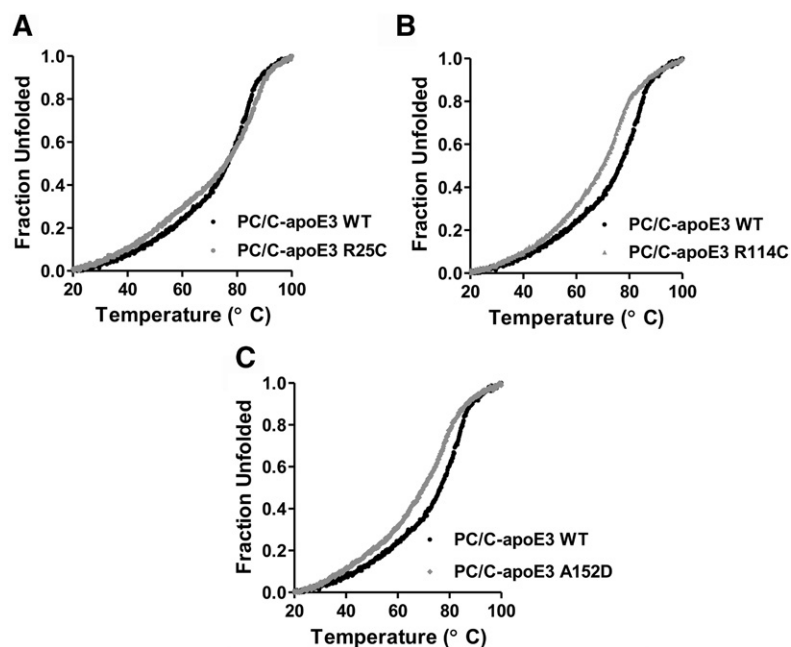


Fig. 7. Effect of R25C, R114C, and A152D mutations on thermal unfolding of apoE3 in reconstituted lipoprotein particles. The thermal denaturation profile of each mutant in PC/cholesterol (C)-apoE particles is presented in comparison to the WT protein. The y-axis has been normalized to correspond to the fraction of the protein in the unfolded state. Four separate experiments were performed.

DISCUSSION

In a previous study, we had suggested that apoE3 variants where a proline residue substituted another residue led to secondary content alterations, thermodynamic destabilization, hydrophobic surface exposure, and aggregation of apoE3 due to secondary structure destabilization resulting from the incompatibility of proline in helical regions (18). Our current study suggests, however, that the destabilization seen in LPG-associated variants is not limited to proline presence, but rather extends to other types of residues, such as Cys and Asp, that are generally compatible with helical regions. The two studies interpreted together rather suggest that specific substitutions in the N-terminal moiety

of apoE3 that lead to secondary structure content changes, thermodynamic destabilization, and hydrophobic surface exposure have the potential of being pathogenic and thus point to a unifying mechanism linking apoE3 mutations and the pathogenesis of LPG. Very rare cases of glomerulopathy, which are different from that of LPG, because they are characterized by marked glomerular foam cell infiltration, have been reported in homozygotes for the apoE2 isoform and, in most of the cases, have been associated with type III hyperlipoproteinemia (41, 42). ApoE2, which harbors the R158C substitution, has similar α -helical content as apoE3 and appears to be more thermodynamically stable compared with apoE3 (36). Therefore, apoE2 is not expected to lead to LPG, explaining the distinct-to-LPG

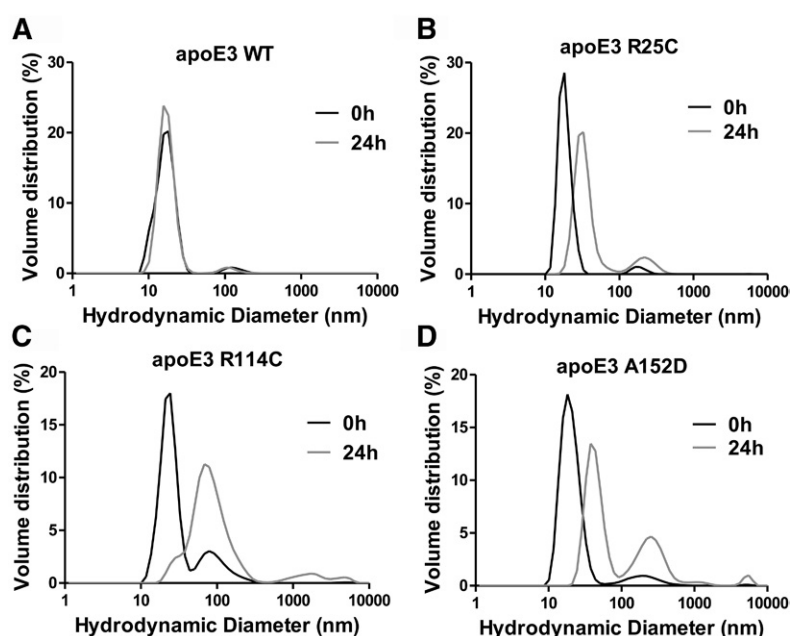


Fig. 8. Effect of R25C, R114C, and A152D mutations on the oligomerization of apoE3. Volume-normalized particle distribution profiles of lipid-free WT and mutant apoE3 forms, measured by DLS. Black line corresponds to 0 h incubation and gray line to 24 h incubation at 37°C. Three separate experiments were performed.

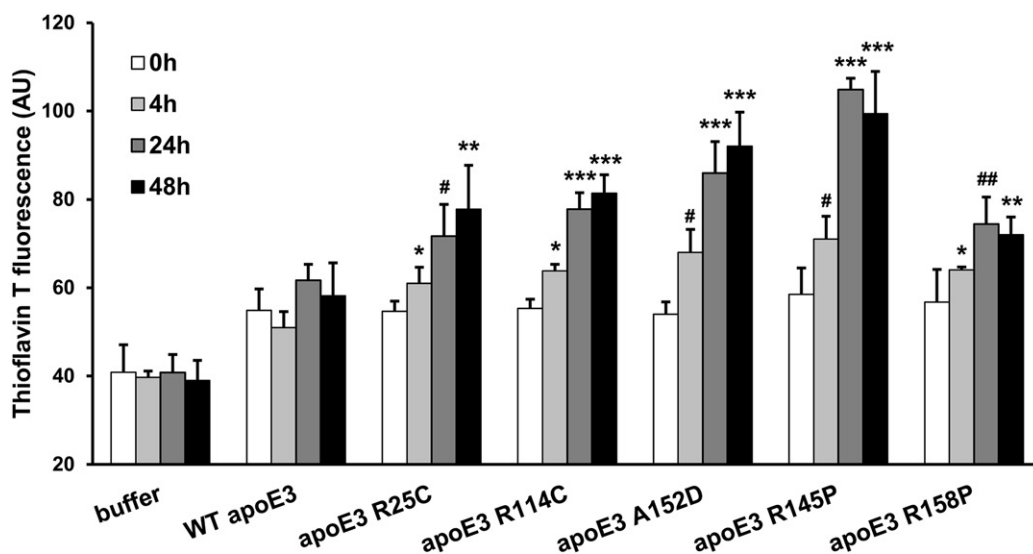


Fig. 9. Effect of various mutations associated with LPG on the capacity of apoE3 to bind to the amyloid probe ThT. ThT was added on WT or mutant apoE3 forms before (0 h) or after their incubation at 37°C for 4, 24, or 48 h, followed by measurement of fluorescent intensity, as described in Materials and Methods. Values represent the means \pm SD ($n = 6$). * $P < 0.05$; # $P < 0.01$; ** $P < 0.005$; ## $P < 0.001$; *** $P \leq 0.0001$ versus WT apoE3 after incubation for 4, 24, or 48 h, respectively; AU, arbitrary units.

phenotype of glomerulopathy rarely reported to apoE2 homozygotes (41, 42). This is supported further by animal studies showing that virus-mediated transduction of apoE2 in apoE^{-/-} mice does not promote LPG-like intraglomerular depositions, in contrast to the presence of LPG-like depositions following apoE_{Sendai} virus injection (26). Furthermore, the observed structural and thermodynamic alterations for all LPG-associated apoE3 mutants described here and in Georgiadou et al. (18) come in contrast to the relatively minor perturbations found for other disease-linked mutations analyzed previously that are also located within the same structural domain (34). ApoE3 variants R136S, R145C, and K146E, which have been associated with type III hyperlipoproteinemia, but not with LPG, display much milder repercussions on apoE3 structure and stability (34), indicating that, although any mutation in this region of apoE3 may be detrimental to its structural and thermodynamic integrity, the specific concerted effects for all LPG-associated apoE3 mutants our group has described may be the result of the particular amino acid substitutions.

Although liver is the major source of apoE in the circulation, apoE is also synthesized by the kidney, with a substantial portion of kidney protein synthesis committed to apoE synthesis (43). Elevated apoE levels have been associated with the onset of glomerulus diseases in rats (44, 45), and it has been proposed that apoE might be a risk factor for glomerulus lesions and renal disease (46). Most of the LPG patients have been reported to present elevated plasma apoE levels (5, 6, 23–25), while it has been observed that normalization or reduction of apoE levels following various treatments (e.g., lipid-lowering treatments with fenofibrate or protein A immunoabsorption) result in remission or improvement of the disease (24, 25, 47). The increased levels of plasma apoE in LPG patients along with the increased mechanical pressure native to the glomerulus during the

normal filtration process that leads to additional elevation of the local apoE levels could enhance the aggregation kinetics of destabilized apoE mutants already susceptible to aggregation. A running hypothesis could be that newly synthesized renal mutant apoE and/or apoE dissociated from lipoproteins may aggregate in glomerular capillaries and due to its increased portion of exposed hydrophobic surfaces associate with lipoproteins and therefore promote the formation of lipoprotein thrombi.

A link between the thermodynamic stability of apoE3 variants, their propensity to aggregate, and the formation of lipoprotein thrombi in the glomerulus suggests that the stabilization of the apoE3 variants may hold possible therapeutic benefit. Indeed, it has been demonstrated that it is possible to stabilize the apoE4 (a common polymorphic variant of apoE) structure using small molecules (48). As a result, the identification of small molecules that can bind to and stabilize LPG-associated apoE3 variants may constitute an interesting approach toward the future development of therapeutics for LPG.

In summary, we have analyzed the thermodynamic and aggregation effects of rare apoE3 mutations that are associated with LPG, a rare renal disease, characterized by lipoprotein thrombi in the glomerular capillaries. Our results, combined with a previous study, provide a unified framework for understanding the potential pathogenic mechanism of these mutations and suggest a putative pathway for the discovery of small-molecule therapeutics for this disease. **■**

The authors thank Drs. G. Kordas and E. K. Efthimiadou (National Center for Scientific Research “Demokritos”, Athens) for assistance with the DLS analysis. Protein production and biophysical analyses were performed using infrastructure that is associated with the Greek National Research Infrastructure in Structural Biology, Instruct-EL.

REFERENCES

1. Saito, T., A. Matsunaga, K. Ito, and H. Nakashima. 2014. Topics in lipoprotein glomerulopathy: an overview. *Clin. Exp. Nephrol.* **18**: 214–217.
2. Tsimihodimos, V., and M. Elisaf. 2011. Lipoprotein glomerulopathy. *Curr. Opin. Lipidol.* **22**: 262–269.
3. Mourad, G., J. P. Cristol, C. Turc-Baron, and A. Djamali. 1997. Lipoprotein glomerulopathy: a new apolipoprotein-E-related disease that recurs after renal transplantation. *Transplant. Proc.* **29**: 2376.
4. Miyata, T., S. Sugiyama, M. Nangaku, D. Suzuki, K. Uragami, R. Inagi, H. Sakai, and K. Kurokawa. 1999. Apolipoprotein E2/E5 variants in lipoprotein glomerulopathy recurred in transplanted kidney. *J. Am. Soc. Nephrol.* **10**: 1590–1595.
5. Matsunaga, A., and T. Saito. 2014. Apolipoprotein E mutations: a comparison between lipoprotein glomerulopathy and type III hyperlipoproteinemia. *Clin. Exp. Nephrol.* **18**: 220–224.
6. Stratikos, E., and A. Chroni. 2014. A possible structural basis behind the pathogenic role of apolipoprotein E hereditary mutations associated with lipoprotein glomerulopathy. *Clin. Exp. Nephrol.* **18**: 225–229.
7. Zannis, V. I., K. E. Kypreos, A. Chroni, D. Kardassis, and E. E. Zanni. 2004. Lipoproteins and atherogenesis. In *Molecular Mechanisms of Atherosclerosis*. Taylor & Francis, Abington, UK. 111–174.
8. Huang, Y. and R. W. Mahley. 2014. Apolipoprotein E: structure and function in lipid metabolism, neurobiology, and Alzheimer's diseases. *Neurobiol. Dis.* **72**(Pt A): 3–12.
9. Zannis, V. I., and J. L. Breslow. 1981. Human very low density lipoprotein apolipoprotein E isoprotein polymorphism is explained by genetic variation and posttranslational modification. *Biochemistry.* **20**: 1033–1041.
10. Mahley, R. W., K. H. Weisgraber, and Y. Huang. 2009. Apolipoprotein E: structure determines function, from atherosclerosis to Alzheimer's disease to AIDS. *J. Lipid Res.* **50**(Suppl): S183–S188.
11. Johnson, L. A., J. M. Arbones-Mainar, R. G. Fox, A. A. Pendse, M. K. Altenburg, H. S. Kim, and N. Maeda. 2011. Apolipoprotein E4 exaggerates diabetic dyslipidemia and atherosclerosis in mice lacking the LDL receptor. *Diabetes.* **60**: 2285–2294.
12. Morrow, J. A., D. M. Hatters, B. Lu, P. Hochtl, K. A. Oberg, B. Rupp, and K. H. Weisgraber. 2002. Apolipoprotein E4 forms a molten globule. A potential basis for its association with disease. *J. Biol. Chem.* **277**: 50380–50385.
13. Hatters, D. M., C. A. Peters-Libeu, and K. H. Weisgraber. 2006. Apolipoprotein E structure: insights into function. *Trends Biochem. Sci.* **31**: 445–454.
14. Chen, J., Q. Li, and J. Wang. 2011. Topology of human apolipoprotein E3 uniquely regulates its diverse biological functions. *Proc. Natl. Acad. Sci. USA.* **108**: 14813–14818.
15. Frieden, C., H. Wang, and C. M. W. Ho. 2017. A mechanism for lipid binding to apoE and the role of intrinsically disordered regions coupled to domain-domain interactions. *Proc. Natl. Acad. Sci. USA.* **114**: 6292–6297.
16. Chetty, P. S., L. Mayne, S. Lund-Katz, S. W. Englander, and M. C. Phillips. 2017. Helical structure, stability, and dynamics in human apolipoprotein E3 and E4 by hydrogen exchange and mass spectrometry. *Proc. Natl. Acad. Sci. USA.* **114**: 968–973.
17. Wilson, C., M. R. Wardell, K. H. Weisgraber, R. W. Mahley, and D. A. Agard. 1991. Three-dimensional structure of the LDL receptor-binding domain of human apolipoprotein E. *Science.* **252**: 1817–1822.
18. Georgiadou, D., K. Stamatakis, E. K. Efthimiadou, G. Kordas, D. Gantz, A. Chroni, and E. Stratikos. 2013. Thermodynamic and structural destabilization of apoE3 by hereditary mutations associated with the development of lipoprotein glomerulopathy. *J. Lipid Res.* **54**: 164–176.
19. Argyri, L., I. Dafnis, T. A. Theodosiou, D. Gantz, E. Stratikos, and A. Chroni. 2014. Molecular basis for increased risk for late-onset Alzheimer disease due to the naturally occurring L28P mutation in apolipoprotein E4. *J. Biol. Chem.* **289**: 12931–12945.
20. Dafnis, I., L. Argyri, M. Sagnou, A. Tzinia, E. C. Tsilibary, E. Stratikos, and A. Chroni. 2016. The ability of apolipoprotein E fragments to promote intraneuronal accumulation of amyloid beta peptide 42 is both isoform and size-specific. *Sci. Rep.* **6**: 30654.
21. Gau, B., K. Garai, C. Frieden, and M. L. Gross. 2011. Mass spectrometry-based protein footprinting characterizes the structures of oligomeric apolipoprotein E2, E3, and E4. *Biochemistry.* **50**: 8117–8126.
22. Huang, R. Y., K. Garai, C. Frieden, and M. L. Gross. 2011. Hydrogen/deuterium exchange and electron-transfer dissociation mass spectrometry determine the interface and dynamics of apolipoprotein E oligomerization. *Biochemistry.* **50**: 9273–9282.
23. Saito, T., Y. Ishigaki, S. Oikawa, and T. T. Yamamoto. 2001. Role of apolipoprotein E variants in lipoprotein glomerulopathy and other renal lipidoses. *Clin. Exp. Nephrol.* **5**: 201–208.
24. Hu, Z., S. Huang, Y. Wu, Y. Liu, X. Liu, D. Su, Y. Tao, P. Fu, X. Zhang, Z. Peng, et al. 2014. Hereditary features, treatment, and prognosis of the lipoprotein glomerulopathy in patients with the APOE Kyoto mutation. *Kidney Int.* **85**: 416–424.
25. Xin, Z., L. Zhihong, L. Shijun, Z. Jinfeng, C. Huiping, Z. Caihong, J. Daxi, and L. Leishi. 2009. Successful treatment of patients with lipoprotein glomerulopathy by protein A immunoabsorption: a pilot study. *Nephrol. Dial. Transplant.* **24**: 864–869.
26. Ishigaki, Y., S. Oikawa, T. Suzuki, S. Usui, K. Magoori, D. H. Kim, H. Suzuki, J. Sasaki, H. Sasano, M. Okazaki, et al. 2000. Virus-mediated transduction of apolipoprotein E (ApoE)-sendai develops lipoprotein glomerulopathy in ApoE-deficient mice. *J. Biol. Chem.* **275**: 31269–31273.
27. Matsunaga, A., J. Sasaki, T. Komatsu, K. Kanatsu, E. Tsuji, K. Moriyama, T. Koga, K. Arakawa, S. Oikawa, T. Saito, et al. 1999. A novel apolipoprotein E mutation, E2 (Arg25Cys), in lipoprotein glomerulopathy. *Kidney Int.* **56**: 421–427.
28. Hagiwara, M., K. Yamagata, T. Matsunaga, Y. Arakawa, J. Usui, Y. Shimizu, K. Aita, M. Nagata, A. Koyama, B. Zhang, et al. 2008. A novel apolipoprotein E mutation, ApoE Tsukuba (Arg 114 Cys), in lipoprotein glomerulopathy. *Nephrol. Dial. Transplant.* **23**: 381–384.
29. Bombardieri, A. S., H. Song, V. D. D'Agati, S. D. Cohen, A. Neal, G. B. Appel, and B. H. Rovin. 2010. A new apolipoprotein E mutation, apoE Las Vegas, in a European-American with lipoprotein glomerulopathy. *Nephrol. Dial. Transplant.* **25**: 3442–3446.
30. Dafnis, I., J. Metso, V. I. Zannis, M. Jauhiainen, and A. Chroni. 2015. Influence of isoforms and carboxyl-terminal truncations on the capacity of apolipoprotein E to associate with and activate phospholipid transfer protein. *Biochemistry.* **54**: 5856–5866.
31. Morrisett, J. D., J. S. David, H. J. Pownall, and A. M. Gotto, Jr. 1973. Interaction of an apolipoprotein (apoLP-alanine) with phosphatidylcholine. *Biochemistry.* **12**: 1290–1299.
32. Gorshkova, I. N., K. Liadaki, O. Gursky, D. Atkinson, and V. I. Zannis. 2000. Probing the lipid-free structure and stability of apolipoprotein A-I by mutation. *Biochemistry.* **39**: 15910–15919.
33. Ekblad, C. M., H. R. Wilkinson, J. W. Schymkowitz, F. Rousseau, S. M. Freund, and L. S. Itzhaki. 2002. Characterisation of the BRCT domains of the breast cancer susceptibility gene product BRCA1. *J. Mol. Biol.* **320**: 431–442.
34. Georgiadou, D., A. Chroni, A. Vezeridis, V. I. Zannis, and E. Stratikos. 2011. Biophysical analysis of apolipoprotein E3 variants linked with development of type III hyperlipoproteinemia. *PLoS One.* **6**: e27037.
35. Clément-Collin, V., A. Barbier, A. D. Dergunov, A. Visvikis, G. Siest, M. Desmadril, M. Takahashi, and L. P. Aggerbeck. 2006. The structure of human apolipoprotein E2, E3 and E4 in solution. 2. Multidomain organization correlates with the stability of apoE structure. *Biophys. Chem.* **119**: 170–185.
36. Morrow, J. A., M. L. Segall, S. Lund-Katz, M. C. Phillips, M. Knapp, B. Rupp, and K. H. Weisgraber. 2000. Differences in stability among the human apolipoprotein E isoforms determined by the amino-terminal domain. *Biochemistry.* **39**: 11657–11666.
37. Aggerbeck, L. P., J. R. Wetterau, K. H. Weisgraber, C. S. Wu, and F. T. Lindgren. 1988. Human apolipoprotein E3 in aqueous solution. II. Properties of the amino- and carboxyl-terminal domains. *J. Biol. Chem.* **263**: 6249–6258.
38. Perugini, M. A., P. Schuck, and G. J. Howlett. 2000. Self-association of human apolipoprotein E3 and E4 in the presence and absence of phospholipid. *J. Biol. Chem.* **275**: 36758–36765.
39. Hatters, D. M., N. Zhong, E. Rutenber, and K. H. Weisgraber. 2006. Amino-terminal domain stability mediates apolipoprotein E aggregation into neurotoxic fibrils. *J. Mol. Biol.* **361**: 932–944.
40. Ramella, N. A., O. J. Rimoldi, E. D. Prieto, G. R. Schinella, S. A. Sanchez, M. S. Jaureguiberry, M. E. Vela, S. T. Ferreira, and M. A. Tricerri. 2011. Human apolipoprotein A-I-derived amyloid: its association with atherosclerosis. *PLoS One.* **6**: e22532.
41. Sakatsume, M., M. Kadamura, I. Sakata, N. Imai, D. Kondo, Y. Osawa, H. Shimada, M. Ueno, T. Miida, S. Nishi, et al. 2001. Novel glomerular lipoprotein deposits associated with apolipoprotein E2 homozygosity. *Kidney Int.* **59**: 1911–1918.
42. Kawanishi, K., A. Sawada, A. Ochi, T. Moriyama, M. Mitobe, T. Mochizuki, K. Honda, H. Oda, T. Nishikawa, and K. Nitta. 2013. Glomerulopathy with homozygous apolipoprotein e2: a report of three cases and review of the literature. *Case Rep. Nephrol. Urol.* **3**: 128–135.

43. Blue, M. L., D. L. Williams, S. Zucker, S. A. Khan, and C. B. Blum. 1983. Apolipoprotein E synthesis in human kidney, adrenal gland, and liver. *Proc. Natl. Acad. Sci. USA.* **80**: 283–287.
44. van Goor, H., M. L. van der Horst, J. Atmosoerodjo, J. A. Joles, A. van Tol, and J. Grond. 1993. Renal apolipoproteins in nephrotic rats. *Am. J. Pathol.* **142**: 1804–1812.
45. Calandra, S., E. Gherardi, M. Fainaru, A. Guaitani, and I. Bartosek. 1981. Secretion of lipoproteins, apolipoprotein A-I and apolipoprotein E by isolated and perfused liver of rat with experimental nephrotic syndrome. *Biochim. Biophys. Acta.* **665**: 331–338.
46. Zhou, T. B. 2013. Signaling pathways of apoE and its role of gene expression in glomerulus diseases. *J. Recept. Signal Transduct. Res.* **33**: 73–78.
47. Wu, H., Y. Yang, and Z. Hu. 2018. The novel apolipoprotein E mutation ApoE Chengdu (c.518TC, p.L173P) in a Chinese patient with lipoprotein glomerulopathy. *J. Atheroscler. Thromb.* **25**: 733–740.
48. Mahley, R. W., and Y. Huang. 2012. Small-molecule structure correctors target abnormal protein structure and function: structure corrector rescue of apolipoprotein E4-associated neuropathology. *J. Med. Chem.* **55**: 8997–9008.